Pedro Henrique Grosman Alves

Mitigation of turbulence-caused random-like perturbations on down-converted photons in atmospheric links.

A dissertation submitted as partial fulfillment of the requirements for the degree of Master of Physics in the physics postgraduate program of the Instituto de Ciências Exatas - UFMG.

Supervisor: Prof. Dr. Carlos Henrique Monken

Belo Horizonte

2019

Dados Internacionais de Catalogação na Publicação (CIP)

A474m Alves, Pedro Henrique Grosman.
Mitigation of turbulence-caused random-like perturbations on down-converted photons in atmospheric links / Pedro Henrique Grosman Alves. – 2019.
46f., enc. : il.

Orientador: Carlos Henrique Monken.

Dissertação (mestrado) – Universidade Federal de Minas Gerais, Departamento de Física.
Bibliografia: f. 43-46.

1. Informação quântica. 2. Óptica quântica. 3. Fótons.
I. Título. II. Monken, Carlos Henrique. III. Universidade Federal de Minas Gerais, Departamento de Física.

CDU – 530.145 (043)

Elaborada pela Biblioteca Professor Manoel Lopes de Siqueira da UFMG.

Universidade Federal de Minas Gerais
Instituto de Ciências Exatas
Programa de Pós-Graduação em Física
Caixa Postal 702
30.123-970 Belo Horizonte - MG - Brasil

Telefone (xx) (31) 3499 5637
(xx) (31) 3499 5633
Fax (xx) (31) 3499 5688
(xx) (31) 3499 5600
e-mail pgfisica@fisica.ufmg.br

ATA DA SESSÃO DE ARGUIÇÃO DA 631ª DISSERTAÇÃO DO PROGRAMA DE PÓS-GRADUAÇÃO EM FÍSICA DEFENDIDA POR PEDRO HENRIQUE GROSMAN ALVES, orientado pelo professor Carlos Henrique Monken para obtenção do grau de **MESTRE EM FÍSICA**. Às 09:00 horas de vinte e três de outubro de 2019, na sala 4129 do Departamento de Física da UFMG, reuniu-se a Comissão Examinadora, composta pelos professores **Carlos Henrique Monken** (Orientador - Departamento de Física/UFMG), **Leonardo Teixeira Neves** (Departamento de Física/UFMG) e **Walber Hugo de Brito** (Departamento de Física/UFMG) para dar cumprimento ao Artigo 37 do Regimento Geral da UFMG, submetendo o bacharel **PEDRO HENRIQUE GROSMAN ALVES** à arguição de seu trabalho de dissertação, que recebeu o título de **"Mitigation of turbulence-caused random-like perturbations on down-converted photons in atmospheric links"**. Às 14:00 horas do mesmo dia o candidato fez uma exposição oral de seu trabalho durante aproximadamente 50 minutos. Após esta, os membros da comissão prosseguiram com a sua arguição e apresentaram seus pareceres individuais sobre o trabalho, concluindo pela aprovação do candidato.

Belo Horizonte, 23 de outubro de 2019.

Prof. Carlos Henrique Monken
Orientador do estudante
Departamento de Física/UFMG

Prof. Leonardo Teixeira Neves
Departamento de Física/UFMG

Prof. Walber Hugo de Brito
Departamento de Física/UFMG

Candidato

Pedro H. Grosman Alves

This work is dedicated to my parents, Carlos Renato Alves and Neide Grosman, and to my children, Miguel Alves, and Gabriela Alves, for always being a source of breath and courage.

Acknowledgements

Foremost, I would like to express my gratitude to my supervisor Prof. Dr. Carlos Henrique Monken for always being motivating, willing and supporting during all steps of the realization of this work.

My sincere thanks also go to my family, an to all my friends for the unconditional love and support.

Last but not least, I thank the Conselho Nacional de Desenvolvimento Científico e Tecnológico (CNPq) for the financial support which made this work possible.

Abstract

Research in optical communication through atmospheric links faces many challenges in seeking for a reliable implementation. Coherent classical light, such as a laser beam propagating through the atmosphere, suffers a significant impact on signal quality due to atmospheric turbulence. Although there are several communication techniques to mitigate signal fading in classical light, any of these techniques do not eliminate the aberrations that come from several sources. Thus, it is worth to develop new techniques to soften even more the turbulence-induced perturbations. In this work, we study an experimental setup to mitigate turbulence-induced signal fluctuations, i.e., signal fading, on entangled photon beams, which leads us to a more stable communication. Twin-photons quantum states, spontaneously produced by parametric-down conversion, were used to demonstrate experimentally that an inversion of transverse coordinates of the correlation beam is sufficient to partially eliminate the aberrations caused by turbulent airflow. Furthermore, we show that not only a coordinate inversion does mitigate turbulence effects, but it completely eliminates the wavefront tilt aberration. Our evaluation reveals that optical communication through atmospheric links could benefit from using quantum states of light.

Keywords: twin-photons, quantum information, correlation beams, atmospheric turbulence.

Resumo

A pesquisa em comunicação óptica por meio de links atmosféricos enfrenta uma série de desafios na busca por uma implementação confiável. A luz clássica coerente, como um feixe de laser propagando-se pela atmosfera por exemplo, sofre um impacto significativo na qualidade do sinal devido à turbulência atmosférica. Embora existam várias técnicas de comunicação para mitigar o desvanecimento do sinal na luz clássica, qualquer uma dessas técnicas não elimina completamente os efeitos indesejados. Assim, vale a pena desenvolver novas maneiras para suavizar ainda mais as perturbações induzidas pela turbulência. Neste trabalho, estudamos um arranjo experimental para mitigar as flutuações de sinal induzidas pela turbulência, ou seja, o desvanecimento do sinal, em feixes de fótons emaranhados, o que nos leva a uma comunicação mais estável. Estados quânticos de fótons gêmeos, espontaneamente produzidos por conversão paramétrica, foram usados para demonstrar experimentalmente que uma inversão das coordenadas transversais do feixe de correlação é suficiente para eliminar parcialmente as perdas de sinal causadas pelo fluxo turbulento de ar. Além disso, mostramos que não apenas uma inversão de coordenadas mitiga os efeitos de turbulência, mas também elimina completamente a aberração da inclinação da frente de onda. Nossa avaliação revela que a comunicação óptica através de canais atmosféricos pode se beneficiar do uso de estados quânticos para luz.

Palavras-chave: fótons gêmeos, informação quântica, feixes de correlação, turbulência atmosférica

Contents

1 Introduction

Quantum physics transformed the way we interpret nature. With the coming of the quantum theory, in addition to incredible discoveries, our understanding of information theory could be rethought. Ever since, representing, transmitting, and processing information using quantum states of physical systems have been showing some particular benefits in comparison with classical systems. David Deutsch, one of the pioneers in quantum computing, proposed in 1985 a quantum algorithm able to solve a mathematical problem that is insoluble by classical operations [1]. Afterward, in 1993, C. H. Bennett and coworkers discovered the quantum teleportation [2], which would be impossible using classical physics. Later, quantum teleportation was experimentally realized in several different forms using optical techniques [3], photon polarization [4], 'squeezed' states of light [5], and using nuclear magnetic resonance [6]. When it comes to transmitting information codified in quantum states safely, we must draw our attention to a fascinating feature. For the first time in history, cryptography has stood on fundamental laws of physics instead of algorithmic securing. [7].

There are several physical systems, such as atoms, and molecules for example, which we can encode information on its quantum states [8, ch. 4] [9]. However, in this text, we refer to quantum states of light only. As S. Barz shows [10], we can embody and process information using quantum states of light and implement quantum information using photonic qubits. G. Leuchs and coworkers, also show how we can perform quantum communication with coherent light states [11].

The light used to encode quantum states can be transmitted through fibre-based channels, as used by many telecommunication companies, and through free-space channels as in via satellite communication. As via satellite communications occur in atmospheric channels, quantum communication through the atmosphere is under intense investigation [12–14]. Compared with fibre-based demonstrations, free-space links could provide the most attractive solution for communication over vast distances.

Since we desire to carry out efficient communication using quantum optics, both seeking for upgrading quantum key distribution equipment and researching in via satellite quantum key distribution for long-distance connections turn relevant.

It is reasonable to think that, in some way and at some degree, the atmospheric conditions can affect the transmission of information. It is a common experience to notice the changing view of distant objects from day to day as atmospheric conditions vary. These varying conditions are caused by factors like rain, snow, sleet, fog, haze, pollution, that can significantly limit our ability to view distant objects. These same factors also affect the transmission of electromagnetic radiation through the atmosphere, particularly optical waves.

Despite the varying conditions caused by other factors, atmospheric turbulence causes wavefront distortion in the optical wave resulting in a *spreading of the beam* (beyond that due to pure diffraction), random variations of the beam centroid's position, which is called *beam wander*, and a random distribution of energy within a cross-section of the beam leading to *irradiance fluctuations*. Besides, the atmospheric turbulence gradually destroys the spatial coherence of a laser beam as it propagates [15]. Unfortunately, these detrimental effects have far-reaching consequences on astronomical imaging, free-space optical communications, remote sensing, laser radar, and other applications that require the transmission of optical waves through the atmosphere.

At this moment, some fair questions may emerge: how to eliminate, or at least minimize, the drawbacks caused by the turbulent atmosphere in quantum optics communication? Is it possible to exploit the quantum nature of light to soften turbulence-like effects? If so, why it would not be possible using classical light?

In 2013, Pereira and coworkers published a paper whose results strongly inspired this dissertation [16]. In that work, the authors introduced a scheme for an odd-order aberration-free transmission through a simulated turbulent atmosphere. Their results showed that it is possible to transmit a two-photon beam with a Gaussian profile through a turbulent-like cell with almost no signal loss.

Although the work carried out by Pereira *et al.* shows interesting results and answers the previous questions, we extend their work by introducing a more straightforward analysis based on profiling coincidence-countings. Our experimental configuration allows us to qualitatively achieve the same mitigation effect as Pereira, but by a different and extended scheme. In our scheme, the inversion of coordinates is made by using prisms instead of using an interferometer-like arrangement, which makes the configuration easier to set up. Moreover, our scheme implements a two-dimensional inversion of coordinates case on both of the twin-photons, which makes our case more general than the one-dimensional case proposed by Pereira [16]. Furthermore, our setup allows us to see the effects of the wavefront tilt aberration and how it can be eliminated.

This text is organized as follows: in Chapter 2, the theoretical foundations necessary to understand this work are introduced. Among the approached topics, parametric down-conversion, angular spectrum propagation, and classical theory for propagation in random

media are discussed briefly. The primary object of this text is outlined in section 2.4, where we introduce our plan for mitigating turbulence-caused aberrations and discuss some questions related to the title of this work as well. In Chapter 3, we both show the experimental setup proposed to accomplish this work and discuss this proposal in details. The results obtained in the laboratory are showed. Finally, in Chapter 4, the exposition of all the conclusions taken from the experimental data and theoretical studies concludes the text.

2 Theory

In this chapter, both the fundamental theoretical results and the main concepts used in this work are presented.

In the following sections, we will regard mainly in exposing the basics of parametric down-conversion theory, angular spectrum propagation, and propagation of optical waves through random media. We only focus on the ideas and results that are interesting for the sake of this work, but additional and more detailed readings will always be suggested.

2.1 Spontaneous parametric down-conversion

The phenomenon called spontaneous parametric down-conversion (SPDC) was first observed by D. Burnham and D. Weinberg in 1970 [17]. This important quantum optics process results from non-linear interactions between electromagnetic fields and material media, generating entangled photon pairs. Describing from a quantum point of view, what occurs is, for example, the spontaneous conversion of one incident photon in two photons with lower energy. The down-converted photons have joint properties, and so are called twin-photons.

There are some excellent works examining the features and the properties of down-converted photon pairs [18–22], and although we can find several texts covering this subject in the quantum optics literature [23, ch. 22] [24, ch. 6] [25], I am going to discuss the SPDC theory briefly.

When an electromagnetic wave propagates through a medium made up of atoms and molecules, the electric charge distribution of this medium suffers a perturbation, in the form of movement, caused by the applied field. This perturbation generates a favored dipole moment orientation and produces in the medium a dipole moment per unit volume $\mathbf{P}$. If the incident radiation field amplitude is similar to the molecular electric field amplitude, then the relation between the polarization of the medium and the incident field will be nonlinear. So, a scalar component of the polarization vector can be written as an expansion of the form:

$$P_i = \epsilon_0 \chi_{ij}^{(1)} E_j + \chi_{ijk}^{(2)} E_j E_k + \chi_{ijkl}^{(3)} E_j E_k E_l + \cdots , \tag{2.1}$$

where $\chi^{(2)}, \chi^{(3)}, \cdots$, are higher order tensors, and Einstein's notation is used [1]. This sort of light-matter interaction brings us in front of a nonlinear optical effect.

[1] According to this notation, when an index variable appears twice in a single term and is not otherwise defined, it implies summation of that term over all the values of the index.

In SPDC, the spontaneously-decayed electrons give rise to two photons simultaneously, producing two output beams named *signal* and *idler*. In summary, in this nonlinear optical process, photons with frequency ω_3 and wave vector $\mathbf{k}_3$ are pumped in a nonlinear bi-refractive crystal generating two photons with frequencies ω_2 and ω_1 and, respectively, wave vectors $\mathbf{k}_2$ and $\mathbf{k}_1$ so that

$$\begin{aligned} \hbar\omega_3 &= \hbar\left(\omega_1 + \omega_2\right), \\ \hbar\mathbf{k}_3 &= \hbar\left(\mathbf{k}_1 + \mathbf{k}_2\right). \end{aligned} \tag{2.2}$$

To satisfy the conservation of momentum inside the nonlinear crystal, certain *phase-matching conditions* must be met [26]. Spontaneous parametric down conversion can be implemented in two different ways, depending on which phase-matching condition was used. If both outgoing photons are ordinary in their polarization, it is deemed as type-I phase matching. If one of the photons is extraordinarily polarized while the other is ordinarily polarized, it is called type-II phase matching. Conservation laws and constraints on polarization determine the possible paths of the outgoing photons. In both cases, the outgoing photons are correlated in their polarization.

The process is said to be degenerate if the down-converted photons have the same frequency (e.g., $\omega_1 = \omega_2 = \omega_3/2$), and nondegenerate otherwise. In general, the photons leaving the crystal propagate in non-collinear directions. However, under certain conditions, the pair may also exit collinearly, in the same direction as the pump.

2.1.1 Two-photon quantum state

In a more formal treatment, we must carry out an electromagnetic field quantization, using a perturbative approach for example, inside the volume Ω of the medium. In such a case, the Hamiltonian is given by

$$\mathcal{H} = \mathcal{H}_0 + \mathcal{H}_I, \tag{2.3}$$

where $\mathcal{H}_0$ is the linear component of $\mathcal{H}$ and the perturbed part of the Hamiltonian $\mathcal{H}_I$ is the nonlinear component, given by

$$\mathcal{H}_I = \frac{1}{2}\int_\Omega \mathbf{E}\cdot\mathbf{P}_{nl}\, d^3\mathbf{r}, \tag{2.4}$$

where $\mathbf{P}_{nl}$ is the nonlinear portion of $\mathbf{P}$. Concerning ourselves only with that portion, we can expand the electric field in terms of plane waves and then adopt the usual method of quantization to find the quantum state produced by SPDC.

The two-photon state generated by collinear-degenerate type-I down-conversion in a nonlinear crystal, neglecting birefringence effects, in the paraxial and monochromatic

approximations, is equal to [21]

$$|\psi\rangle = C_1 |\psi_{vac}\rangle + C_2 \int\int \nu(\mathbf{q}_1 + \mathbf{q}_2) \operatorname{sinc}\left(\frac{L}{4k_p}|\mathbf{q}_1 - \mathbf{q}_2|^2\right) |\mathbf{q}_1\rangle |\mathbf{q}_2\rangle \, d\mathbf{q}_1 d\mathbf{q}_2, \tag{2.5}$$

where $\mathbf{q}_1$ and $\mathbf{q}_2$ are the transverse components of the down-converted wave vectors, $\nu(\mathbf{q}_1 + \mathbf{q}_2)$ is the pump-beam plane-wave spectrum, k_p is the pump-beam wave number, L the crystal thickness, $|\mathbf{q}_1\rangle$ and $|\mathbf{q}_2\rangle$ are one-photon Fock states in plane wave modes, and $|\psi_{vac}\rangle$ represents the zero-photon vacuum state. C_1 and C_2 are such that $|C_2| \ll |C_1|$, and C_2 depends on some parameters as the crystal length, the nonlinearity coefficient, and the magnitude of the pump beam, for example.

The two-photon quantum state in Eq. (2.5) has normalized complex amplitude, that we can take as the normalized angular spectrum of the two-photon field [27] given by

$$\mathcal{A}^{(2)}(\mathbf{q}_1, \mathbf{q}_2) = \langle \mathbf{q}_1 | \langle \mathbf{q}_2 | \psi \rangle = \nu(\mathbf{q}_1 + \mathbf{q}_2) W(\mathbf{q}_1 - \mathbf{q}_2), \tag{2.6}$$

where we can note that $W(\mathbf{q}_1 - \mathbf{q}_2) = \operatorname{sinc}\left(\frac{L}{4k_p}|\mathbf{q}_1 - \mathbf{q}_2|^2\right)$.

We may yet represent the last result in transverse-spatial coordinates $\boldsymbol{\rho}$:

$$\mathcal{A}^{(2)}(\boldsymbol{\rho}_1, \boldsymbol{\rho}_2) = \int\int \nu(\mathbf{q}_1 + \mathbf{q}_2) W(\mathbf{q}_1 - \mathbf{q}_2) \exp\left[i\left(\boldsymbol{\rho}_1 \cdot \mathbf{q}_1 + \boldsymbol{\rho}_2 \cdot \mathbf{q}_2\right)\right] d\mathbf{q}_1 d\mathbf{q}_2. \tag{2.7}$$

Performing a change of variables such that

$$\begin{aligned} \mathbf{P} &= \mathbf{q}_1 + \mathbf{q}_2, \\ \mathbf{Q} &= \mathbf{q}_1 - \mathbf{q}_2, \end{aligned} \tag{2.8}$$

we have

$$\mathcal{A}^{(2)}(\boldsymbol{\rho}_1, \boldsymbol{\rho}_2) = \int\int \nu(\mathbf{P}) W(\mathbf{Q}) e^{i\boldsymbol{\rho}_1 \cdot (\mathbf{P}+\mathbf{Q})/2} e^{i\boldsymbol{\rho}_2 \cdot (\mathbf{P}-\mathbf{Q})/2} \, d\mathbf{P} d\mathbf{Q}, \tag{2.9}$$

or yet

$$\mathcal{A}^{(2)}(\boldsymbol{\rho}_1, \boldsymbol{\rho}_2) = E_p\left(\frac{\boldsymbol{\rho}_1 + \boldsymbol{\rho}_2}{2}\right) V\left(\frac{\boldsymbol{\rho}_1 - \boldsymbol{\rho}_2}{2}\right). \tag{2.10}$$

E_p is the Fourier transform of ν, that is, the pump-beam profile in the nonlinear crystal and V is the Fourier transform of W.

2.2 The angular spectrum and its propagation

The quantum theory which deals with the transverse correlations of photons makes use of some techniques of Fourier Optics, in particular, the propagation of the angular spectrum. Fourier Optics [28] provides a useful method to calculate the propagation of an electromagnetic field through an optical system.

The transfer of angular spectrum from the pump beam to the two-photon state created by SPDC [27] is the basis of some impressive results related to transverse-spatial

correlations. [29–32]. As an example, an interesting point also connected with the transfer of angular spectrum is the question of conservation and entanglement of orbital angular momentum of photons in SPDC [30, 33]. Now, we are about to see what exactly is the angular spectrum of an electromagnetic field.

Considering a monochromatic scalar field $E(\mathbf{r}, t)$ of frequency ω satisfying the homogeneous electromagnetic wave equation, which is harmonic time-dependent, so that $E(\mathbf{r}, t) = E(\mathbf{r})e^{-i\omega t}$, we arrive at the Helmholtz equation:

$$\nabla^2 E(\mathbf{r}) + k^2 E(\mathbf{r}) = 0. \tag{2.11}$$

Here $k^2 = \omega^2 \mu\epsilon$, where μ and ϵ are the magnetic permeability and the dielectric constant of the medium, respectively, and the medium is considered to be dielectric, homogeneous, isotropic, and non-magnetic.

Assuming paraxial waves propagating near the z axis, the transverse field profile can be written as a two-dimensional Fourier integral [28]

$$E(\boldsymbol{\rho}, z) = \int \tilde{E}(\mathbf{q}, z) e^{i\mathbf{q}\cdot\boldsymbol{\rho}}\, d\mathbf{q}, \tag{2.12}$$

where the vectors $\mathbf{q}$ and $\boldsymbol{\rho}$ are the transverse components of $\mathbf{k}$ and $\mathbf{r}$, respectively.

Taking the inverse Fourier transform of the last expression, we have

$$\tilde{E}(\mathbf{q}, z) = \frac{1}{(2\pi)^2} \int E(\boldsymbol{\rho}, z) e^{-i\mathbf{q}\cdot\boldsymbol{\rho}}\, d\boldsymbol{\rho}, \tag{2.13}$$

where the integration domain is the entire xy-plane. $\tilde{E}(\mathbf{q}, z)$ is deemed as the *angular spectrum* of the field [28] [23, ch. 3].

2.2.1 Angular spectrum propagation and the detection amplitude

Now we are going to see see how the angular spectrum modifies with the propagation along the z-axis. Taking the Eq. (2.12) into the Helmholtz equation, we have the following integral to be satisfied:

$$\int \left[-q^2 \tilde{E}(\mathbf{q}, z) + \frac{d^2}{dz^2} \tilde{E}(\mathbf{q}, z) + k^2 \tilde{E}(\mathbf{q}, z) \right] e^{i\mathbf{q}\cdot\boldsymbol{\rho}}\, d\mathbf{q} = 0, \tag{2.14}$$

where $q^2 = k_x^2 + k_y^2$. This, recognizing that $k_z^2 = k^2 - q^2$, leads us to

$$\frac{d^2}{dz^2} \tilde{E}(\mathbf{q}, z) + k_z^2 \tilde{E}(\mathbf{q}, z) = 0. \tag{2.15}$$

The general solution for this differential equation can be written as

$$\tilde{E}(\mathbf{q}, z) = \tilde{E}(\mathbf{q}, 0) e^{\pm i k_z z}, \tag{2.16}$$

where the signals $\pm$ correspond to the angular spectrum propagation along the positive and negative z direction, respectively. Now we can see that the propagation is simply described by the phase factor $e^{\pm ik_z z}$.

Considering only the positive signal and taking (2.16) into (2.12), we find an expression for $E(\boldsymbol{\rho}, z)$ in terms of the angular spectrum at the $z = 0$ plane, that is $\tilde{E}(\mathbf{q}, 0)$:

$$E(\boldsymbol{\rho}, z) = \int \tilde{E}(\mathbf{q}, 0) e^{i\left(\mathbf{q}\cdot\boldsymbol{\rho} + \sqrt{k^2 - q^2}z\right)} \, d\mathbf{q}, \tag{2.17}$$

where the domain of integration is all the plane of spatial frequencies defined by the vector $\mathbf{q}$. Eq. (2.17) can be seen as an expansion of the electromagnetic field in plane waves, which can be homogeneous ($k^2 \geq q^2$) or evanescent ($k^2 < q^2$). In general, we will be interested in long distance fields ($z \gg \lambda$) where the evanescent contribution is absolutely negligible.

The expression (2.17) is the two-dimensional Fourier transform of a product, so we can apply the convolution theorem for Fourier transforms to obtain

$$E(\boldsymbol{\rho}, z) = \int E(\boldsymbol{\rho}', 0) G(\boldsymbol{\rho} - \boldsymbol{\rho}', z) \, d\boldsymbol{\rho}', \tag{2.18}$$

where $E(\boldsymbol{\rho}', 0)$ is the Fourier transform of $\tilde{E}(\mathbf{q}, 0)$, and $G(\boldsymbol{\rho} - \boldsymbol{\rho}', z)$ is the Fourier transform of $e^{i\sqrt{k^2 - q^2}z}$, such that [34]

$$G(\boldsymbol{\rho}, z) = \frac{e^{ik\sqrt{\rho^2 + z^2}z}}{i\lambda(\rho^2 + z^2)} \left(1 + \frac{i}{k\sqrt{\rho^2 + z^2}}\right). \tag{2.19}$$

In order to express $G(\boldsymbol{\rho}, z)$, and then $E(\boldsymbol{\rho}, z)$, in a much simpler form, we must make use of the *Fresnel approximation* [28], and consider $z \gg \lambda$ so that the imaginary part in (2.19) vanishes. By doing this, Eq. (2.18) turns into:

$$E(\boldsymbol{\rho}, z) \simeq \frac{e^{ikz}}{i\lambda z} \int E(\boldsymbol{\rho}', 0) e^{i\frac{k}{2z}|\boldsymbol{\rho} - \boldsymbol{\rho}'|^2} \, d\boldsymbol{\rho}'. \tag{2.20}$$

We can insert Eq. (2.10) in Eq. (2.20) to obtain the two-photon detection amplitude at the point $\mathbf{r}_1 = \mathbf{r}_2 = \mathbf{r} = (\boldsymbol{\rho}, z\hat{\boldsymbol{z}})$:

$$\begin{aligned} \mathcal{A}^{(2)}(\mathbf{r}, \mathbf{r}) \propto \int\int E_p \left(\frac{\boldsymbol{\rho}_1' + \boldsymbol{\rho}_2'}{2}\right) V \left(\frac{\boldsymbol{\rho}_1' - \boldsymbol{\rho}_2'}{2}\right) \\ \times \exp\left[\frac{ik}{2z}\left(|\boldsymbol{\rho}_1' - \boldsymbol{\rho}|^2 + |\boldsymbol{\rho}_2' - \boldsymbol{\rho}|^2\right)\right] d\boldsymbol{\rho}_1' d\boldsymbol{\rho}_2'. \end{aligned} \tag{2.21}$$

Equation (2.21) can be viewed as the paraxial approximation of a superposition of two one-photon spherical-wave originated at the plane $z = 0$ inside the nonlinear crystal at points $\boldsymbol{\rho}_1'$ and $\boldsymbol{\rho}_2'$ with a joint amplitude given by $E_p(\boldsymbol{\rho}_1', \boldsymbol{\rho}_2') V(\boldsymbol{\rho}_1', \boldsymbol{\rho}_2')$.

2.3 Propagation through random media

Laser beam propagation through random media is a subset of generalized wave propagation and scattering in a medium. By random medium, we mean one whose fundamental properties are random functions of space and time. Typical examples include the earth atmosphere, the ocean, and biological media. In this text, we will concern only with weak fluctuations caused by turbulence in an atmospheric medium.

Although a complete theory of wave propagation through random media is not yet available, the general approach is, in certain asymptotic regimes, reasonably well understood, and that is what we concentrate on here. Further reading about propagation of correlation beams in turbulent atmospheres can be found in Avetisyan's [35] and Pereira's [36] thesis works.

2.3.1 Weak and strong fluctuation conditions

First of all, when studying the propagation of electromagnetic waves in random media, we must classify at some degree how strong the turbulence conditions are. All methods used currently for studying this subject, are valid only in a specific regime of turbulence.

Theoretical studies of optical waves propagating under turbulence conditions are conventionally classified as belonging to either weak or strong fluctuations theories. We can use the Kolmogorov spectrum [37, ch. 3] to study plane waves or spherical waves that have propagated over a path of length L, and then distinguish between these cases by values of the *Rytov variance*

$$\sigma_R^2 = 1.23 C_n^2 k^{7/6} L^{11/6}, \tag{2.22}$$

where C_n^2 is the refractive-index structure parameter. *Weak fluctuations* are associated with $\sigma_R^2 < 1$, and then the Rytov variance physically represents the irradiance fluctuations associated with an unbounded plane wave [37, ch. 8]. *Moderate fluctuations* conditions are characterized by $\sigma_R^2 \sim 1$, and *strong fluctuations* are associated with $\sigma_R^2 > 1$.

2.3.2 Classical theory of propagation in random media

When an optical/IR wave propagates through a random medium like the Earth's atmosphere, both the amplitude and phase of the electric field experience random fluctuations caused by small random changes in the index of refraction. Random fluctuations in the refractive index of the atmosphere are directly associated with microscopic temperature fluctuations caused by the turbulent motion of the air due to winds and convection. Although these refractive-index fluctuations are only a few parts in a million, a propagating

optical wave passes through a large number of refractive-index inhomogeneities, so their cumulative effect on the optical wave is quite profound.

Here we introduce the *stochastic Helmholtz equation* as the governing partial differential equation for the scalar field of an optical wave propagating through a random medium. The classical problem of optical wave propagation in an unbounded continuous medium with smoothly varying stochastic refractive index has a governing differential equation with random coefficients [38, 39].

By assuming a harmonic time-variation (monochromatic wave) in the electric field, Maxwell's equations for a propagating electromagnetic wave lead directly to [39, 40]

$$\nabla^2\mathbf{E} + k^2 n^2(\mathbf{r})\mathbf{E} + 2\nabla\left[\mathbf{E}\cdot\log n(\mathbf{r})\right] = 0, \tag{2.23}$$

where $\mathbf{r}$ denotes a point in space, $k = 2\pi/\lambda$ is the wave number of the electromagnetic wave, $n(\mathbf{r})$ is the refractive index whose time variation has been suppressed. $n(\mathbf{r})$ can be viewed as a function of position only by assuming a quasi-steady-state approach, i.e., time variations in the refractive index are sufficiently slow.

The last equation can be reduced to a more rudimentary equation by imposing a couple of fundamental and straightforward assumptions on the propagating wave - both the *backscattering* and *depolarization* effects can be neglected. These two assumptions follow from the same idea: because the wavelength λ for optical radiation is much smaller than the smallest scale of turbulence (i.e., the inner scale l_0) [37, ch. 3], the maximum scattering angle is roughly $\lambda/l_0 \sim 10^{-4}$ rad. It follows that monochromatic radiation scattered by relatively weak, large-scale refractive fluctuations is contained within a narrow cone about the forward scatter in the propagation direction. As a further consequence, the last term on the left-hand side of equation (2.23) is negligible [39, 41]. Dropping this term, which is related to the change in polarization of the wave as it propagates, the equation (2.23) simplifies to

$$\nabla^2\mathbf{E} + k^2 n^2(\mathbf{r})\mathbf{E} = 0. \tag{2.24}$$

Equation (2.24) is now easily decomposed in three scalar equations, one for each component of the field $\mathbf{E}$. Let $E(\mathbf{r})$ denotes the scalar component that is transverse to the direction of propagation along the positive z-axis, then (2.24) modifies to the scalar *stochastic Helmholtz equation*

$$\nabla^2 E(\mathbf{r}) + k^2 n^2(\mathbf{r})E(\mathbf{r}) = 0. \tag{2.25}$$

Even with the above simplifications, equation (2.25) has proven to be hardly solvable. One of the first approaches to solve it was based on the method of Green's function, reducing (2.25) to an equivalent integral equation. Although exact solutions of (2.25) by any method have never been found, some more useful attempts to solve this

equation were based both on the geometrical optics method, which ignores diffraction effects, and on two perturbation theories widely know as the *Born approximation* [37, ch. 5] and *Rytov approximation* [37, ch. 5].

2.3.3 Born approximation

The governing stochastic equation we desire to solve is Eq. (2.25). One of the most conventional approaches to solve this equation is the Born approximation, based on the addition of perturbing terms to the unperturbed field.

Let us first write the square of the refractive index as

$$n^2(\mathbf{r}) = [n_0 + n_1(\mathbf{r})]^2 \cong 1 + 2n_1(\mathbf{r}), \quad |n_1(\mathbf{r})| \ll 1. \tag{2.26}$$

We have assumed that the mean value satisfies $n_0 = \langle n(\mathbf{r}) \rangle \cong 1$ and that $n_1(\mathbf{r})$ is a small random quantity with null mean value. If the optical wave is propagating along the positive z-axis, the transverse scalar components of the field at $z = L$ can be expressed as a sum of terms:

$$E(\mathbf{r}) = E_0(\mathbf{r}) + E_1(\mathbf{r}) + E_2(\mathbf{r}) + \cdots, \tag{2.27}$$

where $E_0(\mathbf{r})$ denotes the unscattered part of the field in the absence of turbulence and the remaining terms represent higher-order scattering, caused by random inhomogeneities. Although it may not occur in all propagation problems, it is reasonable assuming that $|E_2(\mathbf{r}, L)| \ll |E_1(\mathbf{r}, L)| \ll |E_0(\mathbf{r}, L)|$. Now, we substitute the last two equations into (2.25) and then equate terms of the same order to reduce the stochastic Helmholtz equation to a system of equations:

$$\nabla^2 E_0 + k^2 E_0 = 0, \tag{2.28a}$$

$$\nabla^2 E_1 + k^2 E_1 = -2k^2 n_1(\mathbf{r}) E_0(\mathbf{r}), \tag{2.28b}$$

$$\nabla^2 E_2 + k^2 E_2 = -2k^2 n_1(\mathbf{r}) E_1(\mathbf{r}), \tag{2.28c}$$

and so on for higher-order terms.

One of the significant advantages of the above perturbation method is that we have transformed an equation with random, space-dependent coefficients in one homogeneous equation and a system of non-homogeneous equations, all with constant coefficients. The solution of the homogeneous equation is, of course, the unperturbed field $E_0(\mathbf{r})$ [37, ch. 4], at the same time that each of the nonhomogeneous equations can be solved by the method of Green's function.

2.3.4 Rytov approximation

A different perturbative approach for solving (2.25) is well-known as the Rytov approximation. The Rytov method, restricted to weak fluctuation conditions, consists of writing the scalar component of an electromagnetic field as

$$E(\mathbf{r}, L) = E_0(\mathbf{r}, L)e^{\psi(\mathbf{r},L)}, \tag{2.29}$$

where $\psi(\mathbf{r}, L)$ is a complex phase perturbation due to turbulence such that

$$\psi(\mathbf{r}, L) = \psi_1(\mathbf{r}, L) + \psi_2(\mathbf{r}, L) + \cdots . \tag{2.30}$$

It is convenient referring to ψ_1 and ψ_2 as the first and second-order complex phase perturbations, respectively.

We may insert Eq. (2.29) directly into (2.25) and then work on developing formal expressions for the first-order and second-order perturbations. Another approach is to relate these perturbations terms directly to the terms *already calculated* in the Born approximation. To do so, we introduce here the *normalized Born perturbations* defined by

$$\Phi_m(\mathbf{r}, L) = \frac{E_m(\mathbf{r}, L)}{E_0(\mathbf{r}, L)}, \quad m = 1, 2, 3 \cdots . \tag{2.31}$$

Equating the first-order Rytov and first-order Born perturbative terms according to

$$\begin{aligned} E_0(\mathbf{r}, L)e^{\psi_1(\mathbf{r},L)} =& E_0(\mathbf{r}, L) + E_1(\mathbf{r}, L) \\ =& E_0(\mathbf{r}, L)\left[1 + \Phi_1(\mathbf{r}, L)\right], \end{aligned} \tag{2.32}$$

we find that the first-order Rytov perturbation is equal to the normalized first-order Born perturbation, i.e.,

$$\begin{aligned} \psi_1(\mathbf{r}, L) =& \log\left[1 + \Phi_1(\mathbf{r}, L)\right] \\ \simeq& \Phi_1(\mathbf{r}, L), \qquad |\Phi_1(\mathbf{r}, L)| \ll 1. \end{aligned} \tag{2.33}$$

2.3.5 Zernike Polynomials and atmospheric effects on imaging systems

In analyzing the effects of turbulence on imaging systems, it is advantageous to represent the phase of the perturbed optical wave in a series of simple orthogonal functions.

The *Zernike polynomials*, introduced by F. Zernike in 1934 [42], represent a set of functions of two variables that are orthogonal over a unit-radius circle. It is usual to define these polynomials as a product of two functions, one depending only on a radial coordinate ρ and the other depending only on the angular coordinate θ, i.e.,

$$Z_n^m(\rho, \theta) = R_n^m(\rho)e^{im\theta}, \tag{2.34}$$

where both m and n are integers, $n \geq 0$, $-n \leq m \leq n$, and $n \pm |m|$ is even. The radial polynomial $R_n^m(\rho)$ is a special case of hypergeometric polynomial that is normalized so that $R_n^m(1) = 1$. It is defined by

$$R_n^m(\rho) = \sum_{k=0}^{(n-|m|)/2} \frac{(-1)^k (n-k)!}{\left(\frac{n+m}{2}-k\right)!\left(\frac{n-m}{2}-k\right)!} \frac{\rho^{n-2k}}{k!}. \tag{2.35}$$

We can see from Eq. (2.35) that the radial polynomial is n-degree and contains no power of ρ less than $|m|$, where m relates to the angular dependence. It is worth to notice that the polynomial is even if m is even and odd if m is odd. The orthogonality property of these polynomials is written as

$$\int_0^1 \int_0^{2\pi} Z_n^m(\rho,\theta) Z_l^{m*}(\rho,\theta) \rho \, d\theta \, d\rho = \frac{\pi}{n+1} \delta_{nl}, \tag{2.36}$$

where $*$ denotes complex conjugate, and δ_{nl} is the Kronecker delta defined by $\delta_{nl} = 0 \, (n \neq l)$ and $\delta_{nl} = 1 \, (n = l)$.

One of the primary uses of the Zernike polynomials is to represent fixed aberrations in optical systems in the form of a generalized Fourier series in Zernike polynomials. Lower-order Zernike polynomials are then referred to by such names as *piston*, *tilt*, *focus*, *astigmatism*, *coma*, and so forth. By using these polynomials, many researchers have been able to study how aberrations affect various imaging systems [43–45]. They are also useful in adaptive optics systems designed for atmospheric turbulence decomposition [46–48].

Any realistic wave front $\Phi(\rho,\theta)$ can be represented in a two-dimensional series of Zernike polynomials over a unit-radius circle:

$$\Phi(\rho,\theta) = \sum_{n=0}^{\infty} \sum_{m=-n}^{n} C_{mn} R_n^m(\rho) e^{im\theta}. \tag{2.37}$$

To obtain the coefficients C_{mn} in the last expression, we first multiply both sides by $\rho R_k^{|m|}(\rho) e^{-im\theta}$ and then integrate over the unit disk. This action leads to

$$\begin{aligned} \int_0^1 \int_0^{2\pi} \rho \Phi(\rho,\theta) R_k^{|m|}(\rho) e^{-im\theta} \, d\theta \, d\rho &= \sum_{n=0}^{\infty} \sum_{m=-n}^{m=n} C_{mn} \int_0^1 \int_0^{2\pi} \rho R_n^{|m|}(\rho) R_k^{|m|}(\rho) \, d\theta \, d\rho \\ &= \frac{\pi}{k+1} \sum_{m=-k}^{k} C_{mk}. \end{aligned} \tag{2.38}$$

As an example, for $k = 0$ we obtain the coefficient for the piston term simply given by the average value of the wave front $\Phi(\rho,\theta)$:

$$C_{00} = \frac{1}{\pi} \int_0^1 \int_0^{2\pi} \rho \Phi(\rho,\theta) \, d\theta \, d\rho = \langle \Phi(\rho,\theta) \rangle . \tag{2.39}$$

Similarly, the coefficient for tilt is obtained by setting $k = 1$ and $m = 1$, which gives us

$$C_{11} = \frac{2}{\pi} \int_0^1 \int_0^{2\pi} \rho^2 \Phi(\rho,\theta) e^{-i\theta} \, d\theta \, d\rho. \tag{2.40}$$

In analyzing the effects of atmospheric turbulence on a propagating optical wave, it can be useful expressing the turbulence-induced random phase perturbations on $\Phi(\rho, \theta)$ in a series of Zernike polynomials.

A modification of the Zernike polynomials (2.34) that is commonly used in studying atmospheric effects on imaging systems leads to Zernike functions defined by

$$\begin{aligned} Z_i(\rho) &\equiv Z_i[0, n] = \sqrt{n+1} R_n^0(\rho), \quad m = 0, \\ Z_{i,even}(\rho, \theta) &\equiv Z_{i,even}[m, n] = \sqrt{n+1} R_n^m(\rho) \sqrt{2} \cos m\theta, \quad m \neq 0, \\ Z_{i,odd}(\rho, \theta) &\equiv Z_{i,odd}[m, n] = \sqrt{n+1} R_n^m(\rho) \sqrt{2} \sin m\theta, \quad m \neq 0. \end{aligned} \tag{2.41}$$

The ordering scheme for these polynomials uses the rule that, for a given n, we count the modes with smaller m first. For $m > 0$, there are two Zernike functions for each (m, n) pair as given in (2.41). The functions Z_i are ordered such that even i correspond to symmetric modes, while odd i match to antisymmetric ones. You can find further and more complete reading about Zernike polynomials and its properties, and how it is related to turbulence-caused aberrations as well, by consulting references [37, ch. 14] [49]. To illustrate, we list the first few polynomials in Table 1.

	Azimuthal frequency (m)		
Radial degree (n)	0	1	2
0	$Z_1 = 1$ Constant		
1		$Z_2 = 2\rho\cos\theta$ $Z_3 = 2\rho\sin\theta$ Tilts (Lateral position)	
2	$Z_4 = \sqrt{3}(2\rho^2 - 1)$ Defocus (Longitudinal position)		$Z_5 = \sqrt{6}\rho^2 \sin 2\theta$ $Z_6 = \sqrt{6}\rho^2 \cos 2\theta$ Astigmatism (3rd Order)

Table 1 – First few Zernike polynomials. The modes Z_i are ordered such that even i corresponds to the symmetric modes defined by $\cos m\theta$, while odd i corresponds to antisymmetric modes given by $\sin m\theta$.

2.4 Aberration canceling

Some fair questions that might emerge at this point are: how a two-photon beam propagates under atmospheric turbulence? Does the atmosphere affect the correlations between entangled photons? If so, is there any possible way to eliminate the drawbacks? These are the major questions of this work, and we will answer them in the following lines.

2.4.1 Propagation of two-photon state in turbulence

Propagation of correlations is a subset of a more general theory called *coherence theory of scalar wavefields*, and you can find further reading on it in Ref. [23, ch. 4]. From now we concern with adding to Eq. (2.21) the influences of the fluctuating refractive index caused by atmospheric turbulence. To do so, a random variable ψ, as proposed in Rytov approximation, is introduced:

$$\begin{aligned}\mathcal{A}_T^{(2)}(\mathbf{r},\mathbf{r}) \propto \int\int E_p\left(\frac{\boldsymbol{\rho}_1'+\boldsymbol{\rho}_2'}{2}\right) V\left(\frac{\boldsymbol{\rho}_1'-\boldsymbol{\rho}_2'}{2}\right) \\ \times \exp\left[\frac{ik}{2z}\left(|\boldsymbol{\rho}_1'-\boldsymbol{\rho}|^2+|\boldsymbol{\rho}_2'-\boldsymbol{\rho}|^2\right)\right] \\ \times \exp\left[\psi(\boldsymbol{\rho}_1',\boldsymbol{\rho};k)+\psi(\boldsymbol{\rho}_2',\boldsymbol{\rho};k)\right]\, d\boldsymbol{\rho}_1' d\boldsymbol{\rho}_2',\end{aligned} \tag{2.42}$$

where the random variable represents a distortion, both in phase and amplitude, of a spherical wave with wave number k originated at $\mathbf{r}' = (\boldsymbol{\rho}', 0\hat{\boldsymbol{z}})$ and observed at $\mathbf{r} = (\boldsymbol{\rho}, z\hat{\boldsymbol{z}})$. In order to simplify Eq. (2.42), it is time to make some assumptions and statements.

In section (2.1) we defined the function $V(\boldsymbol{\rho}_1' - \boldsymbol{\rho}_2')$ as the Fourier transform of $W(\mathbf{q}_1,\mathbf{q}_2) = \mathrm{sinc}\left(\frac{L}{4k_p}|\mathbf{q}_1-\mathbf{q}_2|^2\right)$. If we consider that the nonlinear crystal is thin enough, the function W is broad in $|\mathbf{q}_1-\mathbf{q}_2|$ such that its Fourier transform V can be approximated by a delta function $\delta(\boldsymbol{\rho}_1'-\boldsymbol{\rho}_2')$. Indeed, the nonlinear crystal thickness L is typical of just a few millimetres, which makes this approximation reasonable. Accounting for those assumptions in Eq. (2.42) and solving for one variable of integration we have

$$\mathcal{A}_T^{(2)}(\mathbf{r},\mathbf{r}) \propto \int E_p(\boldsymbol{\rho}') \exp\left[\frac{ik}{z}|\boldsymbol{\rho}'-\boldsymbol{\rho}|^2\right] \exp\left[2\psi(\boldsymbol{\rho}',\boldsymbol{\rho};k)\right]\, d\boldsymbol{\rho}'. \tag{2.43}$$

Taking into consideration again the theory previously exposed in section (2.1), it becomes easy to see that due to the conservation of momentum, $k_p = 2k$. Here we must remember that k is the wave number of each one of the down-converted photons, and k_p is the wave number of the laser-pump beam. This way, the last expression turns into an interesting one:

$$\mathcal{A}_T^{(2)}(\mathbf{r},\mathbf{r}) \propto \int E_p(\boldsymbol{\rho}') \exp\left[\frac{ik_p}{2z}|\boldsymbol{\rho}'-\boldsymbol{\rho}|^2\right] \exp\left[2\psi(\boldsymbol{\rho}',\boldsymbol{\rho};k_p)\right]\, d\boldsymbol{\rho}'. \tag{2.44}$$

From this form of expressing (2.42), we can see that the two-photon beam under turbulence behaves the same way the pump beam would under the same conditions. This transfer of transverse profile, in the absence of turbulence, to the correlation beam was demonstrated by Monken and coauthors in 1998 [27].

Now we can show that the turbulence effects captured by the modelling in Rytov approximation can be mitigated. Coming back to expression (2.10), and carrying out an inversion of transverse-coordinates in one of the photons, for instance, $\mathbf{q}_2 \to -\mathbf{q}_2$, after

repeating the same steps as before we arrive at an expression for the amplitude of detection at the points $\mathbf{r} = (\boldsymbol{\rho}, z\hat{\mathbf{z}})$ and $\tilde{\mathbf{r}} = (-\boldsymbol{\rho}, z\hat{\mathbf{z}})$:

$$\begin{aligned}\mathcal{A}_T^{(2)}(\mathbf{r}, \tilde{\mathbf{r}}) \propto \int E_p(\boldsymbol{\rho}') \exp\left[\frac{ik_p}{2z}|\boldsymbol{\rho}' - \boldsymbol{\rho}|^2\right] \\ \times \exp\left[\psi(\boldsymbol{\rho}', \boldsymbol{\rho}; k) + \psi(-\boldsymbol{\rho}', -\boldsymbol{\rho}; k)\right] d\boldsymbol{\rho}'.\end{aligned} \tag{2.45}$$

To see that the turbulence-induced total random perturbation is symmetric and how the antisymmetric part vanishes, let us write the argument of the second exponential function in Eq. (2.45) in terms of Zernike functions. That gives us

$$\psi(\rho, \theta) + \psi(\rho, \theta + \pi) = \sum_{n=0}^{\infty} \sum_{m=-n}^{n} C_{mn} Z_n^m(\rho, \theta) + \sum_{n=0}^{\infty} \sum_{m=-n}^{n} C_{mn} Z_n^m(\rho, \theta + \pi), \tag{2.46}$$

where the rotation $\theta \to \theta + \pi$ represents the coordinate inversion $\boldsymbol{\rho} \to -\boldsymbol{\rho}$. It is easy to see from Eq. (2.34) that $Z_n^m(\rho, \theta) = (-1)^m Z_n^m(\rho, \theta + \pi)$, which leads us to a summation over the symmetric polynomials only, i.e., even m:

$$\psi(\rho, \theta) + \psi(\rho, \theta + \pi) = \sum_{n=0}^{\infty} \sum_{m_{even}} C_{mn} Z_n^m(\rho, \theta) + \sum_{n=0}^{\infty} \sum_{m_{even}} C_{mn} Z_n^m(\rho, \theta). \tag{2.47}$$

Now, looking at Eq. (2.45), we can easily notice that the antisymmetric part of ψ vanishes. In other words, we can say that the total perturbation is now symmetric to the z-axis.

Another way to achieve the last result is through executing an inversion of coordinates on each photon, but this time the inversion will occur on only one of the two transverse coordinates. Once that we have made an inversion of one coordinate on one of the photons, we must invert the orthogonal coordinate on the other photon. For example, we can perform an inversion such that

$$\begin{aligned}\mathbf{r} &= -x\hat{\mathbf{x}} + y\hat{\mathbf{y}} + z\hat{\mathbf{z}}, \\ \tilde{\mathbf{r}} &= +x\hat{\mathbf{x}} - y\hat{\mathbf{y}} + z\hat{\mathbf{z}}.\end{aligned} \tag{2.48}$$

This way, the antisymmetric part of ψ vanishes again.

3 Experiment

The main purpose of this chapter is to introduce the experimental schemes we have used to subject down-converted photons to turbulence-like conditions. To analyze how random-phase perturbations disrupt the coincident detection of entangled photons, and how inversion of coordinates helps to soften the effects of that kind of perturbation, two different arrangements have been proposed.

Firstly, we performed an analysis using a turbulent chamber to emulate atmospheric air flow. Subsequently, we introduced slight tilts on a mirror to see how the wavefront tilt aberration plays a bad role in detecting twin-photons.

3.1 Mitigation of turbulence effects

There are many ways to simulate atmospheric conditions inside a laboratory [50]. The results described in this work were obtained using the same turbulence emulator as in Pereira's work [36, ch. 2], which is similar to that described in Ref. [51].

The emulator mixes air at different temperatures - the same mechanism which generates turbulence in the atmosphere. Consequently, the refractive index inside the box fluctuates in both space and time [39, ch. 2]. The mixing is made inside an aluminum box, the turbulence chamber, as sketched in Fig. 1. Optical beams pass through the chamber by two holes made along the z-axis. Two coolers are positioned on each side of the box, blowing and exhausting the air within. In front of one of the air injectors, a resistor bank, connected to a stabilized power supply, warms the incoming air by dissipating power. Each dissipated power corresponds to a different turbulence strength, which is already characterized [16].

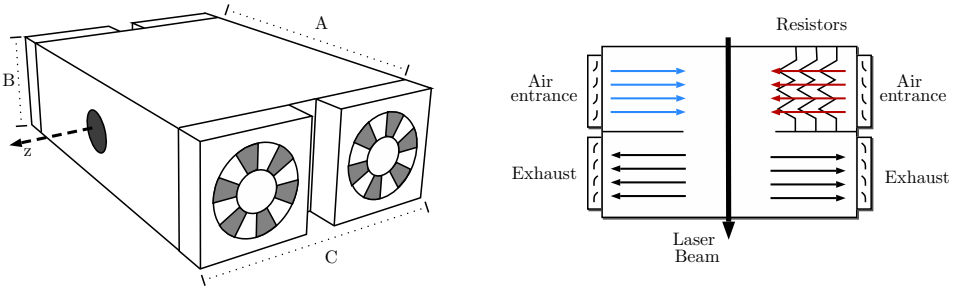

Figure 1 – Turbulence chamber's scheme that emulates the turbulent mixing of air at different temperatures in the atmosphere. Dimensions are $A = 24.5$ cm, $B = 8.5$ cm, and $C = 19.0$ cm. The resistors bank has a net resistance of $6.7\,\Omega$, and is driven by an adjustable power supply that can provide voltages up to 40.0 V and currents of 10.0 A.

Qualitative experimental verification of the expressions (2.44) and (2.45) was made. The main experimental setup is depicted in Fig. 2. A two-photon beam with 790 nm wavelength is produced by collinear type-II SPDC in a 7-mm long β-BaB_2O_4 (BBO) nonlinear crystal (NLC). The pump beam used has 395 nm wavelength and is generated by a frequency-doubling BiB_3O_6 (BIBO) crystal. The BIBO crystal is pumped by a 790 nm-tuned titanium-sapphire laser (120 fs of pulse width) outputting 3.6 W of average power. The quantum state produced in this case differs from that in Eq. (2.5) only by the fact that, in type-II SPDC, one photon is extraordinarily polarized.

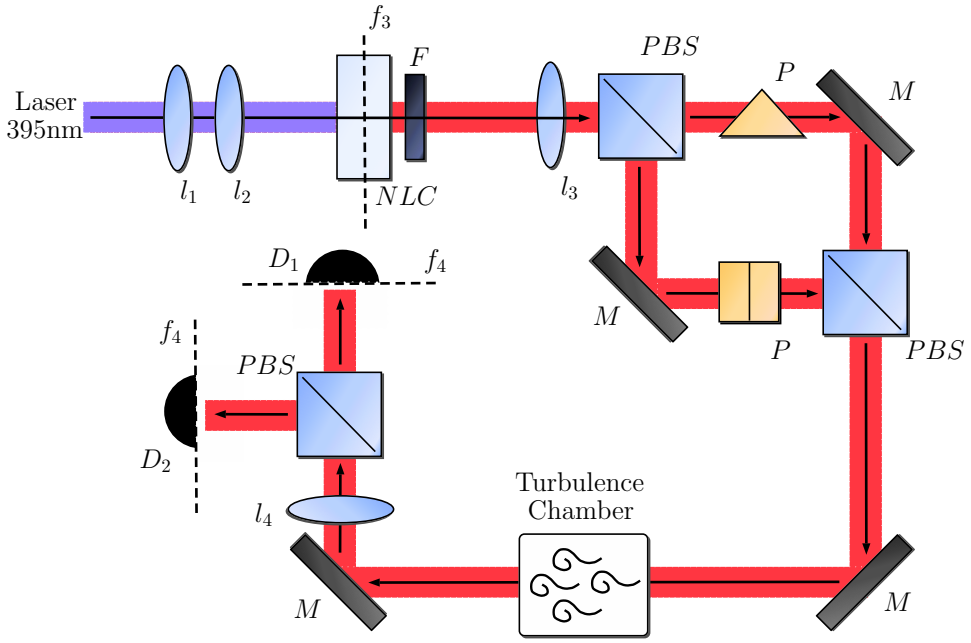

Figure 2 – Experimental setup. The two-photon source consists of lenses l_1, l_2, l_3, the uv filter F, and the nonlinear crystal NLC. The two prisms P are responsible for coordinate inversion. The detection system is made by a lens l_4, a polarizing beam splitter PBS, and two photon counters D_1 and D_2.

Two positive confocal lenses l_1 and l_2 of focal length $f_1 = 50.0$ mm and $f_2 = 125.0$ mm, respectively, are placed at a distance of 400.0 mm, measured from l_2 to NLC, and are responsible for expanding the pump-beam profile. As a result, the laser beam is relatively broad inside the crystal. In order to block the pump-beam, a UV filter F is positioned right beside the crystal.

The third lens l_3 has a focal length of 125.0 mm and is placed 220.0 mm from NLC. The lenses set $l_3 - l_4$ forms a telescope which projects the image of f_3 on the detection plane over D_1 and D_2, f_4. In the case of spatially entangled photons, the position and the momentum observables correspond to measurements in the near and in the far-field, relative to the source plane, namely the SPDC crystal. The near field is associated with position correlations at the source plane, while the far field is associated with momentum correlations at the source plane [21].

All photons arising from the nonlinear crystal were made to propagate through a Mach-Zehnder-like arrangement, where each photon propagates in a different arm depending on its polarization. The two-photon (coincidence) detection profile is made by two fibre-coupled avalanche photodiode detectors, 50 μm-diameter aperture, operating in photon counting mode with a coincidence-resolving time of 5 ns. Bandpass filters centered at 790 nm with 11 nm bandwidth are coupled in front of each detector.

In a first experiment, any of the photons did not undergo inversion of coordinates, and they were not subjected to turbulence as well. By counting the number of coincidences on a small region in the focal plane of l_4, over a sampling time of 20 s, we were able to profile the transverse coincidence countings. This profile is depicted as a heatmap of coincidence countings in Fig. 3A.

The profile showed in Fig. 3A has such a form due to a couple of reasons. First of all, as we have used a pulsed laser, the frequency spread of the detectable down-converted photons is not so small in comparison with the central frequency, so that the dispersion of the refractive index around the central frequency is appreciable [21]. Another point is that, in type-II phase matching, the equations for the two-photons detection amplitude predict different transverse and longitudinal walk-off for ordinary and extraordinary down-converted photons [21]. Otherwise, the profile depicted in Fig. 3A would follow the form of the pump-beam profile inside the nonlinear crystal, according to Eq. (2.42).

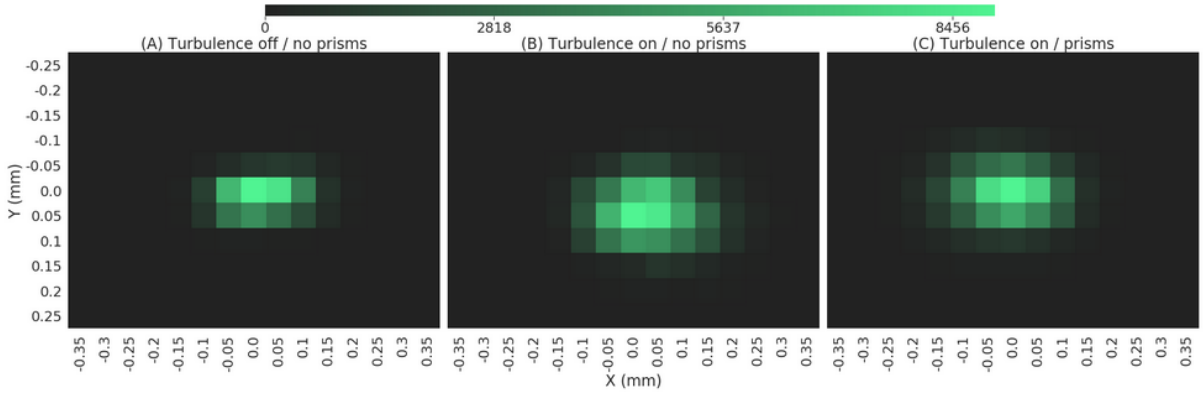

Figure 3 – Transverse coincidence counting profile over 20 s of sampling time. (A) Coincidence profile without influence of turbulence. (B) Coincidence profile under influence of turbulence. (C) Coincidence profile under influence of turbulence after positioning the prisms.

As a second observation, with no prisms again, we placed the turbulence chamber just as showed in Fig. 2. Driving the resistor bank by 20.0 V, approximately 59.7 W of net power is dissipated as heat to warm the incoming air. This way, the down-converted photons were subjected to simulated turbulence, and then we ran the process of counting coincidences again. The twin-photons under the influence of turbulence, in this case, have a coincidence profile as depicted in Fig. 3B.

Subsequently, the major measurement of this experiment was made. By positioning the prisms P, as shown in Fig. 2, both of the photons which pass through one of the two possible paths in the interferometer-like arrangement, undergo a coordinate inversion. The turbulence chamber was used in the same way as before. As we can see from Fig. 2, the photon that passes through one of the arms has one of its transverse coordinates inverted, while the other undergoes an inversion on the orthogonal coordinate. In this sense, this is the same kind of coordinate inversion as shown in Eq. (2.48).

According to Eq. (2.45), we would expect to see a softening of turbulence effects after applying a coordinates inversion. Although the influences of turbulent air flow are not completely eliminated, we can see a reasonable correction in Fig. 3C, and that is partially what we expected. As we can see from Eq. (2.47), even though we have eliminated the antisymmetric part of the turbulence-induced random perturbation, the symmetric part of it remains.

To get a more quantitative insight on how both the simulated turbulence and the addition of the prisms act on the correlation beam, we depicted the normalized one-dimensional coincidence profile as ploted in Fig. 4. The green markers represent experimental data, and the full black lines represent the fitted Gaussian functions.

Our approach is based on evaluating the parameter σ, which is directly related to the dispersion of the set of data values for each curve. For a given σ, for instance the x or y profile under no influence of turbulence, we evaluate both how the random perturbations affect this parameter and how the addition of the two prisms cuts down that effects. Considering the three y profiles in Fig. 4, we can see that in the first case, Fig. 4-B, $\sigma = (42.33 \pm 0.15)\,\mu$m. After turning on the turbulence chamber and positioning the prisms, Fig. 4-D,F, the parameter σ modifies to $\sigma = (71.52 \pm 1.65)\,\mu$m and $\sigma = (60.60 \pm 0.72)\,\mu$m, respectively. As a result, a correction of about 36.7% is achieved in the y profile. On the other hand, we can see no correction in the x profile. We may attribute this lack of correction to the fact that the net-aberration generated in the x direction is not induced by the turbulence chamber; it com from another source, such as instability of laser beam, for example.

Although we barely see any correction in both directions, it is worth noticing that, after positioning the prisms, the beam's centroid returned to the origin of the coordinate system, which is to say that the beam wandering effect was removed. Our results and evaluations suggest that turbulence-mitigation effects can be achieved but, for future experimentation, setup improvements are needed.

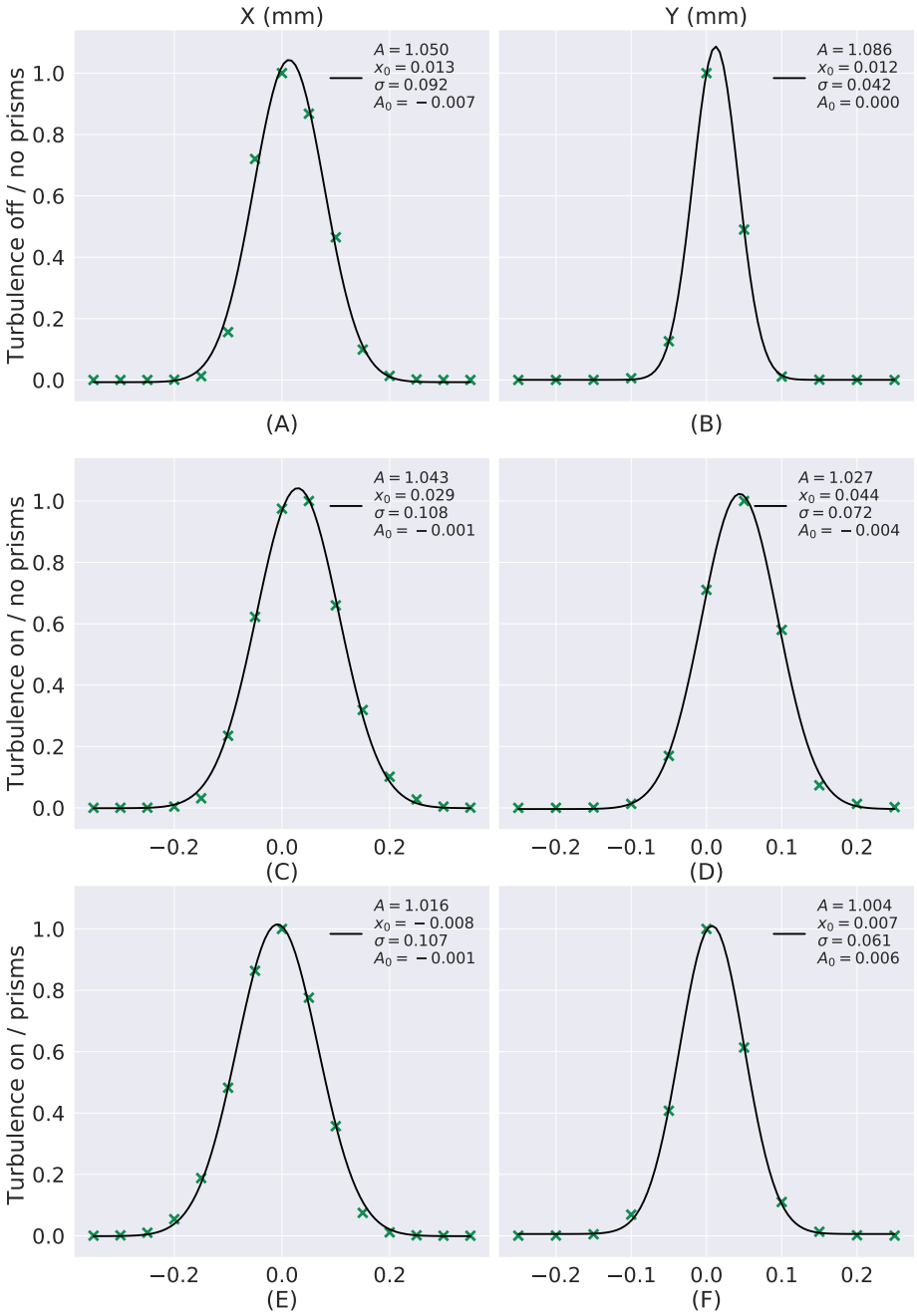

Figure 4 – Normalized one-dimensional coincidence counting profile referring to Fig. 3. All data were fitted by $f(x) = A + A_0 e^{[(x-x_0)/\sigma]^2}$, where x denotes position and $f(x)$ denotes the normalized number of counting.

3.2 Cancellation of wavefront tilt

Among the aberrations caused by atmospheric turbulence, such as beam wandering, scintillation, etc., wavefront tilt has long been deemed as the harmest aberration in terms of spatial resolution [52, 53], accounting for more than 80% of the total distortion.

To investigate how wavefront tilt affects the coincidence detection profile, we introduce in our setup a tilt-adjustable mirror as sketched in Fig. 5. Two piezoelectric devices (PZT) are coupled behind the mirror support to adjust both x and y-direction tilt slightly. In order to simulate random-like perturbation on the wavefront of the twin-photons, each PZT is driven by a function signal generator which generates 1Hz sinusoidal electric signals.

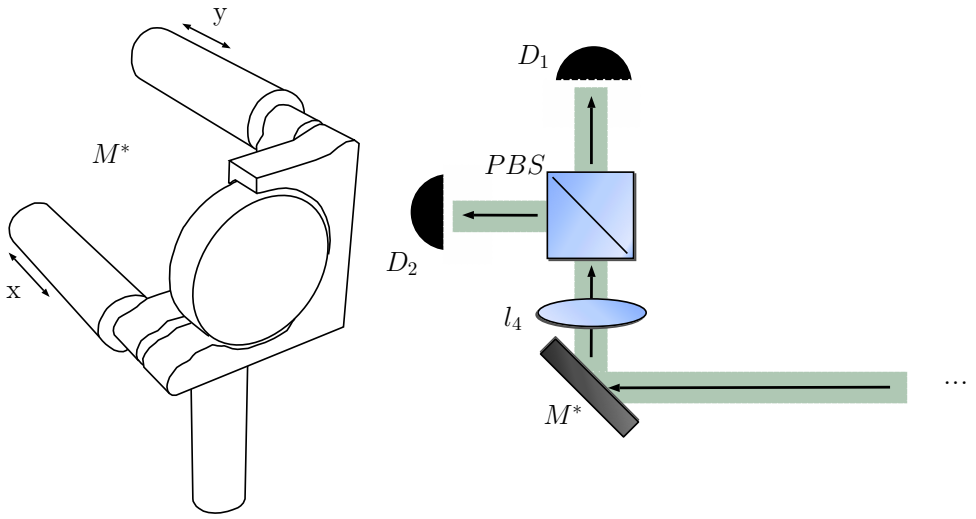

Figure 5 – Sketch of the tilt-adjustable mirror. Each PZT is driven by out of phase sinusoidal electric signals. This configuration was used to simulate random-like wavefront tilt perturbations.

Analogously as we did in the last experiment for mitigating turbulence effects, in the current case, we have made three different observations. Firstly, we have simply profiled the transverse coincidences, without adding any prisms or random-perturbations just as we did in the first experiment. The results are shown in Fig. 6A. Figs. 6B-C show the results after adding the tilt-adjustable mirror and the prisms, respectively.

As we can see from Fig. 6, the inversion of coordinates plays an important role in canceling the drawbacks caused by random-tilt perturbations. The profile of the random-tilted wavefront, as depicted in Fig. 6B, is stretched in the horizontal direction, at the same time that it is a bit more stretched in the vertical direction, almost as if the first figure were separated into two parts. After adding the prisms, Fig. 6C, the first profile is almost retrieved.

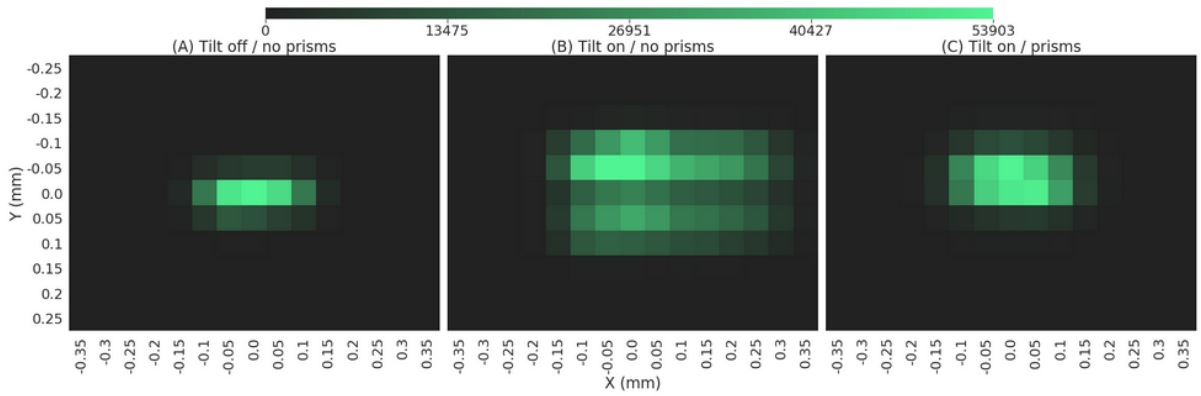

Figure 6 – Transverse coincidence counting profile over 20 s of sampling time. (A) Coincidence profile without influence of wavefront tilt. (B) Coincidence profile under influence of wavefront tilt. (C) Coincidence profile under influence of wavefront tilt after placing the prisms.

Analogously to the previous case, we evaluate the parameter σ under influence of wavefront tilt as depicted in Fig. 7. Considering the three y profiles in Fig. 7, we can see that in the first case, Fig. 7-B, $\sigma = (38.06 \pm 0.06)\,\mu$m. After driving tilt to the mirror and positioning the prisms, Fig. 7F, the parameter σ modifies to $\sigma = (43.31 \pm 1.90)\,\mu$m; which represents about 92.5% of correction. An analogous procedure lead us to conclude that we have achieved 90.7% of correction in the x profile.

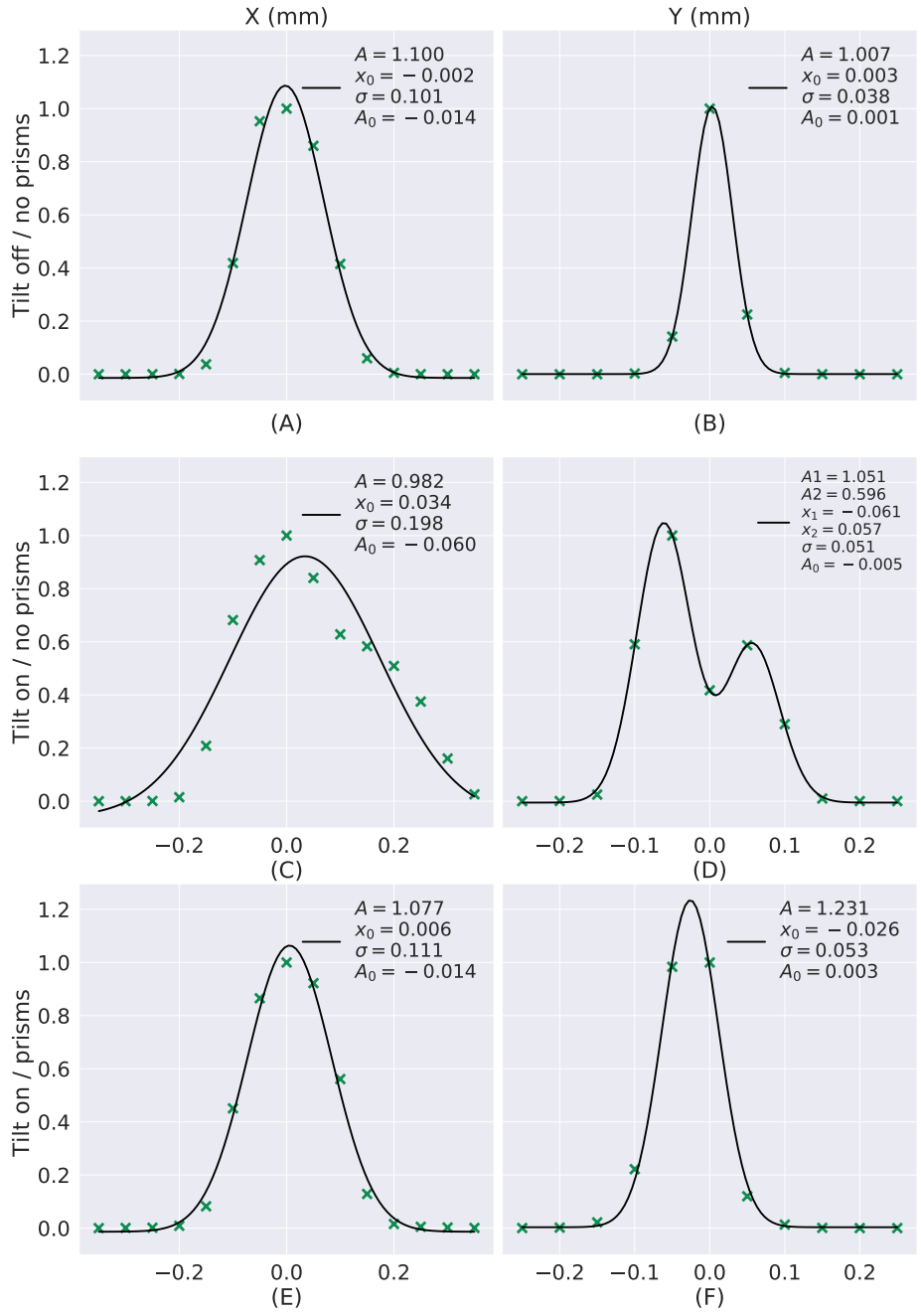

Figure 7 – Normalized one-dimensional coincidence counting profile referring to Fig. 6. All data, except that in figure (D), were fitted by $f(x) = A + A_0 e^{[(x-x_0)/\sigma]^2}$, where x denotes position and $f(x)$ denotes the normalized number of counting. The curve showed in (D) was fitted by $f(x) = A_0 + A_1 e^{[(x-x_1)/\sigma]^2} + A_2 e^{[(x-x_2)/\sigma]^2}$.

4 Concluding Remarks

We studied an experimental setup to mitigate turbulence-induced signal fading in optical communications using twin-photons quantum states. Our experimental configuration allowed us to achieve, in a qualitative manner, approximately the same level of mitigation effect as Pereira [16] using an extension of his setup. The use of prisms to perform inversion of coordinates made our configuration simpler to setup. Moreover, we have implemented a more general case based on a two-dimensional profile analysis. Furthermore, our tilt-adjustable setup allowed us to see the effects of the wavefront tilt aberration on the transverse profile and how it is mitigated, or almost eliminated, by inversion of coordinates.

According to Ref. [52, 53] the wavefront tilt accounts for approximately 80% of the total wavefront distortion. As we could perceive, our experimentation did not show this level of correction when we used the prisms to cancel the signal fading caused by the turbulence chamber. It leads us to think that the turbulence chamber, as it was built, does not simulate atmospheric turbulence very well.

An interesting question, also pointed out in Ref. [16], that may arise is whether entanglement is actually necessary to attain the cancellation effect observed. In Ref. [54] it is demonstrated that, for a known transfer function, classical correlations can be engineered such that it reproduces any joint detection probability attainable in a single plane with entangled photons. Since the channel transfer function changes unpredictably due to turbulence, one would need to continuously monitor it in order to have its form determined, in the same lines of adaptive optics. In our case, the necessary conditions are the transfer of angular spectrum from the pump beam to the down-converted two-photon field.

Although some improvements are needed, our results suggest that spatial-mode entanglement can be protected against turbulence when two-photon states are transmitted through the atmosphere. It is hoped that this work will inspire future research and developments in the use of quantum light for free-space optical communications.

Bibliography

[1] Deutsch, D.: *Quantum theory, the church-turing principle and the universal quantum computer*. In *Proceedings of the Royal Society of London A*, pages 97–117, 1985. Cited on page 15.

[2] Bennette, C. H., G. Brassard, C. Crépeau, R. Jozsa, A. Peres, and W. K. Wootters. *Phys. Rev. Lett.*, 70:1895–1899, 1993. Cited on page 15.

[3] Boschi, D., S. Branca, F. D. Martini, L. Hardy, and S. Popescu. *Phys. Rev. Lett.*, 80:1121–1125, 1998. Cited on page 15.

[4] Bouwmeester, D., J. W. Pan, K. Mattle, M. Eibl, H. Weinfurter, and A. Zeilinger. *Nature*, 390:575–579, 1997. Cited on page 15.

[5] Furusawa, A., J. L. Sørensen, S. L. Braunstein, C. A. Fuchs, Kimble H, J, and E. S. Polzik. *Science*, 282:706–709, 1998. Cited on page 15.

[6] Nielsen, M. A., E. Knill, and R. Laflamme. *Nature*, 396:52–55, 1998. Cited on page 15.

[7] Ma, X.: *Quantum cryptography: from theory to practice*. PhD thesis, Department of Physics, University of Toronto, Toronto, Canada, 2008. `https://arxiv.org/pdf/0808.1385.pdf`. Cited on page 15.

[8] Oliveira, I. S., T. J. Bonagamba, R. S. Sarthour, J. C. Freitas, and E. R. de Azevedo: *NMR Quantum Information Processing*. Elsevier Science B.V., 2007. Cited on page 15.

[9] Blat, L. and C. F. Roos. *Nat. Phys.*, 8:277–284, 2012. Cited on page 15.

[10] Barz, S. *J. Phys. B*, 48:083001, 2015. Cited on page 15.

[11] Khan, I., D. Elser, T. Dirmeier, C. Marquardt, and G. Leuchs. *Philos. Trans. R. Soc. Lond. A*, 375:20160235, 2017. Cited on page 15.

[12] Wang, J. Y. *et al. Nat. Phot.*, 7:387–393, 2013. Cited on page 15.

[13] Nauerth, S., F. Moll, M. Rau, C. Fuchs, J. Horwath, S. Frick, and H. Weinfurter. *Nat. Phot.*, 7:382–386, 2013. Cited on page 15.

[14] Vasylyev, D. Y., A. A. Semenov, and W. Vogel. *Phys. Rev. Lett.*, 108:220501, 2012. Cited on page 15.

[15] Ali, R. N., J. M. Jassim, K. M. Jasim, and M. K. Jawad. *Int. J. Appl. Eng. Res.*, 12:14789–14796, 2017. Cited on page 16.

[16] Pereira, M. V., L. A. P. Filpi, and C. H. Monken. *Phys. Rev. A*, 88:053836, 2013. Cited 3 times on pages 16, 33, and 41.

[17] Burnham, D. C. and D. L. Weinberg. *Phys. Rev. Lett.*, 25:84–87, 1970. Cited on page 19.

[18] Monken, C. H.: *Geração de luz com estatística de fótons sub-Poissoniana, a partir da conversão paramétrica descendente*. PhD thesis, Department of Physics, Universidade Federal de Minas Gerais, Belo Horizonte, Brazil, 1993. Cited on page 19.

[19] Ribeiro, P. H. Souto: *Estudo de propriedades de coerência da luz produzida na conversão paramétrica descendente*. PhD thesis, Department of Physics, Universidade Federal de Minas Gerais, Belo Horizonte, Brazil, 1995. Cited on page 19.

[20] Walborn, S. P.: *The brothers Q: multimode entangled photons with parametric down conversion*. PhD thesis, Department of Physics, Universidade Federal de Minas Gerais, Belo Horizonte, Brazil, 2004. `http://lilith.fisica.ufmg.br/posgrad/Teses_Doutorado/decada2000/stephen-walborn`. Cited on page 19.

[21] Walborn, S.P., C.H. Monken, S. Pádua, and P.H. Souto Ribeiro. *Phys. Rep.*, 495:87–140, 2010. Cited 4 times on pages 19, 21, 34, and 35.

[22] Santos, I. F., L. Neves, G. Lima, C. H. Monken, and S. Pádua. *Phys. Rev. A*, 72:033802, 2005. Cited on page 19.

[23] Mandel, L. and E. Wolf: *Optical coherence and quantum optics*. Cambridge U. Press, 1995. Cited 3 times on pages 19, 22, and 30.

[24] Klyshko, D. N.: *Photons and Nonlinear Optics*. New York: Gordon and Breach, 1988. Cited on page 19.

[25] Hong, C. K. and L. Mandel. *Phys. Rev. A*, 31:2409–2418, 1985. Cited on page 19.

[26] Dmitriev, V., G. Gurzadyan, and D. Nikoyosyan: *Principles of adaptive optics*. New York: Springer-Verlag, 1999. Cited on page 20.

[27] C.H. Monken, P.H. Souto Ribeiro and S. Pádua. *Phys. Rev. A*, 57:3123–3126, 1998. Cited 2 times on pages 21 and 30.

[28] Goodman, J. W.: *Introduction to Fourier Optics*. Boston : Mc Graw Hill, 1996. Cited 3 times on pages 21, 22, and 23.

[29] Fonseca, E. J. S., P.H. Souto Ribeiro, S. Pádua, and C. H. Monken. *Phys. Rev. A*, 60:1530–1533, 1999. Cited on page 22.

[30] Walborn, S. P., A. N. de Olivera, R. S. Thebaldi, and C. H. Monken. *Phys. Rev. A*, 69:023811, 2004. Cited on page 22.

[31] Walborn, S. P., D. S. Ether, R. L. de Matos Filho, and N. Zagury. *Phys. Rev. A*, 76:033801, 2007. Cited on page 22.

[32] Jabir, M. V., N. Apurv Chaitanya, A. Aadhi, and G. K. Samanta. *Sci. Rep.*, 6:21877, 2016. Cited on page 22.

[33] Arnaut, H. H. and G. A. Barbosa. *Phys. Rev. Lett*, 85:286–289, 2000. Cited on page 22.

[34] Stark, H.: *Application of Optical Fourier Transforms*. Orlando: Academic Press, 1982. Cited on page 23.

[35] Avetisyan, H.: *Propagation of Higher Order Correlation Beams in Turbulent Atmosphere*. PhD thesis, Department of Physics, Universidade Federal de Minas Gerais, Belo Horizonte, Brazil, 2016. `http://lilith.fisica.ufmg.br/posgrad/Teses_Doutorado/decada2010/hakob-avetisyan/HakobAvetisyan-tese.pdf`. Cited on page 24.

[36] Cunha Pereira, M.V. da: *Propagação de feixes ópticos de correlação em atmosfera turbulenta*. PhD thesis, Department of Physics, Universidade Federal de Minas Gerais, Belo Horizonte, Brazil, 2014. `http://lilith.fisica.ufmg.br/posgrad/Teses_Doutorado/decada2010/marcelo-pereira/MarceloVitor-tese.pdf`. Cited 2 times on pages 24 and 33.

[37] Andrews, L. C. and R. L. Phillips: *Laser beam propagation through random media*. SPIE Press, 2005. Cited 4 times on pages 24, 25, 26, and 29.

[38] Chernov, L.A.: *Wave Propagation in a Random Medium*. New York : MacGraw-Hill, 1960. Cited on page 25.

[39] Strohbehn, J.W.: *Laser Beam Propagation in the Atmosphere*. New York : Springer, 1978. Cited 2 times on pages 25 and 33.

[40] Ishimaru, A.: *Propagation and Scattering in Random Media*. New Jersey : IEEE Press, 1997. Cited on page 25.

[41] Strohbehn, J. W. *Proceedings of the IEEE*, 56:1301–1318, 1968. Cited on page 25.

[42] Zernike, F. *Physica*, 1:689–704, 1934. Cited on page 27.

[43] Wang, J. Y. and D. E. Silva. *Appl. Opt.*, 19:1510–1518, 1980. Cited on page 28.

[44] Harbers, G., P. J. Kunst, and G. W. R. Leibbrandt. *Appl. Opt.*, 35:6162–6172, 1996. Cited on page 28.

[45] Liang, J., B. Grimm, S. Goelz, and J. F. Bille. *J. Opt. Soc. Am. A*, 11:1949–1957, 1994. Cited on page 28.

[46] Tyson, R. K.: *Principles of adaptive optics*. San Diego: Academic Press, 1991. Cited on page 28.

[47] Driggers, R. G., P. Cox, and T. Edwards: *Introduction to Infrared and Electro-Optical Systems*. Boston: Artech House, 1999. Cited on page 28.

[48] Shapiro, J. H., B. A. Capron, and R. C. Harney. *Appl. Opt.*, 20:3292–3313, 1981. Cited on page 28.

[49] Noll, R. J. *J. Opt. Soc. Am.*, 73:207–211, 1976. Cited on page 29.

[50] Jolissaint, L. *Pubs. Astr. Soc. Pac.*, 118:1205–1224, 2006. Cited on page 33.

[51] Keskin, O., L. Jolissaint, and C. Bradley. *Appl. Opt.*, 45:4888–4897, 2006. Cited on page 33.

[52] Fried, D. L. *J. Opt. Soc. Am.*, 55:1427–1435, 1965. Cited 2 times on pages 38 and 41.

[53] Fried, D. L. *J. Opt. Soc. Am.*, 56:1372–1379, 1966. Cited 2 times on pages 38 and 41.

[54] Bennink, R. S., S. J. Bentley, and R. W. Boyd. *Phys. Rev. Lett.*, 89:113601, 2002. Cited on page 41.